Available online at www.sciencedirect.com
ScienceDirect
Thermochimica Acta 462 (2007) 45–55
thermochimica acta
www.elsevier.com/locate/tca

Enhancement of fluid thermal conductivity by the addition of single and hybrid nano-additives

Soumen Jana, Amin Salehi-Khojin, Wei-Hong Zhong *

Department of Mechanical Engineering and Applied Mechanics, North Dakota State University, Fargo, ND 58105, United States

Received 25 January 2007; received in revised form 26 June 2007; accepted 28 June 2007
Available online 5 July 2007

Abstract

The inherent high thermal conductivity of many nanomaterials has a great potential for enhancing fluidic heat transfer applications. Conductive nanomaterials such as carbon nanotubes (CNTs), copper nanoparticles (CuNPs) and gold nanoparticles (AuNPs), as well as their hybrids such as CNT–CuNP or CNT–AuNP were used in this study to enhance the thermal conductivity of fluids. Mono-type nanoparticle suspensions showed the greatest enhancement in thermal conductivity, among which the enhancement with CuNPs was the highest. Hybrid suspensions did not show the same degree of improvement. The experimentally measured thermal conductivities of several nanofluids were consistently greater than the theoretical predictions obtained from existing models. Mechanisms for the thermal conductivity enhancement are discussed. The stability of nanofluids was estimated by UV–vis–NIR spectrophotometer and it was observed that the stability was influenced by characteristics of nanoparticles.

Keywords: Thermal conductivity; Nanofluid; Nanomaterial; UV–vis–NIR spectrum

1. Introduction

In many engineering fields such as power generation, automobiles, air conditioning, and microelectronics, cooling systems work on a fluid medium such as air, water, mineral oil, or ethylene glycol, through forced flow and/or convectional heat transfer. Heat transfer by convection process depends in part upon thermal conductivity of the fluid. Therefore, improving performance in these engineering applications can be achieved through increasing the thermal conductivity of the fluid. It has been known for a long time, that a suspension of solid particles in a fluid offers a great potential for improvement of heat transfer since thermal conductivity of solids is generally higher than that of fluid (except for mercury) [1]. Different kinds of metallic, non-metallic and polymeric particles can be added to a fluid to make such slurries. However, the size of the particles in micro- and greater-scales can lead to precipitation, abrasion and clogging in the flow path of the fluid. Developments in nanotechnology have introduced a new kind of fluid termed as nanofluid [1]. Nanoparticles (<100 nm) have a better chance to be well dispersed in convectional heat transfer fluid and have shown enhancements in heat transfer [2–6].

In 1991, carbon nanotubes (CNTs) were discovered by Iijima [7]. Single-wall carbon nanotubes (SWNTs) are made of inclined cylindrical graphene plane, while multi-wall carbon nanotubes (MWNTs) have a number of concentric cylinders. Earlier studies found that CNTs have high thermal conductivity and with the potential to be ideal components for heat transfer [8,9]. But some research studies showed very different results. Xie et al. [10] experimented with MWNTs/water, MWNTs/glycol and MWNTs/decene, and did not find any impressive results (only 20% increment with 1 vol.% loading), as Choi et al. [4] found with nanofluid made from MWNTs and synthetic poly(α-olefin) oil. The enhancement of thermal conductivity of MWNTs and synthetic poly(α-olefin) oil nanofluid at 1 vol.% MWNT loading was as high as 160% and depended on volume fraction of MWNTs non-linearly. Assael et al. [11] obtained the same kind of result.

Studies of nanofluid containing other conductive nanofillers have been carried out, and in particular the results from nanofluids containing different metallic and metallic oxide nanoparticles are encouraging. In earlier times, more experiments were performed on thermal properties of nanofluids containing metallic oxide nanoparticles. Masuda et al. [12]

* Corresponding author. Tel.: +1 701 231 7139; fax: +1 701 231 8913.
E-mail address: Katie.Zhong@ndsu.edu (W.-H. Zhong).

0040-6031/$ – see front matter © 2007 Elsevier B.V. All rights reserved.
doi:10.1016/j.tca.2007.06.009

reported that the addition of 4.3 vol.% Al_2O_3 nanoparticles to water increased thermal conductivity of the nanofluid by 30%. Lee et al. [2] worked on the same nanofluid but did not find similar enhancement of thermal conductivity. One of the reasons for this behavior was believed to be the size of the nanoparticles; the size in Masuda's experiment was 13 nm whereas in Lee's experiment it was 33 nm. CuO nanoparticles were added to water and ethylene glycol to produce nanofluids and found enhancement of thermal conductivity. This enhancement was higher compared to the nanofluid having nano-scaled Al_2O_3 [2,13] with the same vol.% of the nanoparticles. While working on CuO, Zhou et al. [13] found more enhancements compared to what was observed by Lee et al. [2] and this enhancement behavior can not be related to particle size as the size of CuO in Zhou et al. experiment was ∼50 nm, whereas in case of Lee et al., the size of nanoparticles was 36 nm.

Nanofluid containing 0.3 vol.% copper nanoparticles (CuNPs) with mean diameter ∼10 nm and ethylene glycol as the fluid showed higher thermal conductivity compared to nanofluid containing same vol.% CuO and same fluid [14]. These studies showed anomalous results considering the effect of size, shape and thermal conductivity of the nanoparticles [15]. The nanofluids with addition of 0.011 vol.% silver nanoparticles (AgNPs) and gold nanoparticles (AuNPs) in water and toluene separately were also studied, which showed enhancement in thermal conductivity of up to 21% [16]. Effect of temperature and surface coatings on thermal properties of nanofluid was observed by Das et al. [17]. Many studies on thermal conductivity of nanofluids having single types of nanofillers were reported [18,19].

Thermal conductivity enhancements of nanofluids with the same composition reported by different literature are not consistent [7–17]. In the process of nanofluid synthesis, timescale of measurements on which stability of nanofluid depends could be the cause for the discrepancy in reported results from the same kind of nanofluids. Also factors such as dispersion of nanoparticles and sizes which influence Brownian motion and interfacial properties should be taken into account to compare the thermal properties of nanofluids from same materials. Liu [20] showed that the thermal conductivity increased ratio for copper–water nanofluids was 23.8% with volume fraction of copper 0.1%. The corresponding Cu nanoparticles were about 50–100 nm and their shapes were spherical and square. It is also reported that variation of shapes in nanoparticles such as from sphere to needle shape would influence the thermal conductivity of nanofluid. With size of around 250 nm and volume fraction of 0.2%, needle shaped Cu nanoparticles showed 3.6% increment in water suspension [20]. It also reports that the thermal conductivity decreases significantly with time variation at the early stages of experiment. Eastman et al. [14] showed that the thermal conductivity of Cu–ethylene glycol nanofluid containing 0.3 vol.% Cu nanoparticles (size, 10 nm) was 40% higher compared to pure ethylene glycol.

From the above discussion, it can be speculated that the enhancement in thermal conductivity of a nanofluid containing two or more component materials may not be estimated by conventional methods. Though several mechanisms have been proposed to validate the experimental results, exact mechanisms for the thermal transport of different medium in nanofluids is still not known. Most of the current methods were constructed considering classical theory applied to micro/macro-scale particles which are totally different from nano-scale particles. Therefore, more experimental work and studies on thermal conductivity of the nanofluids containing different types of nanoparticles are needed to reveal the common causes. CNTs can produce efficient networks in fluid due to their high aspect ratio whereas CuNPs or AuNPs with their small spherical shape can gain Brownian motion in a fluid. Their high specific surface area promotes enhanced thermal conductivity. As a result, both together in a fluid may enhance the thermal conductivity of the nanofluid preserving their own behaviors. It is also possible that their mechanisms may diminish each others effect or one will dominate others, and so the study of the hybrid nanofluid (combination of more than one type nanoparticle in fluid) is a vital component of this work. Successful application of high thermal conductive nanofluids could bring advantages to industry by decreasing the energy consumption and scale of a heat transport function.

In this study, several nanoparticles, oxidization treated CNTs, AuNPs and CuNPs were added to water individually to fabricate single-filler nanofluids. We prepared hybrid nanofluids by adding two types of nanofillers into water: CNT–AuNP and CNT–CuNP, respectively. Thermal conductivities of these nanofluids were measured and analyzed. One of the objectives of this study was to determine the most effective type of nanofillers to achieve the highest thermal conductivity of the nanofluid. Another objective was to study the synergistic effect of nanoparticles on the thermal conductivity of a nanofluid. A third objective was to understand the reasons for the enhancement or decrement of the thermal conductivity of nanofluids.

2. Experiment

CNTs (10 nm in diameter and 5–10 μm in length) were purchased from Catalytic Materials Co., Gold colloidal (AuNP colloidal) was purchased from Sigma–Aldrich Co., Copper nanoparticles (CuNPs) were provided by Materials Modification, Inc., Laurate salt was purchased from Sigma–Aldrich Co.

SEM (Hitachi S-4200 scanning electron microscope) and TEM (JEOL 100CX II transmission electron microscope) images as received from CNTs are shown in Fig. 1. For better dispersion, CNTs were polarized by chemical treatment. One gram of CNTs were suspended in 40 ml of a mixture of concentrated nitric acid and sulfuric acid (1:3 v/v) and refluxed at 140 °C for 1 h. CNTs were filtered from acid solution and washed with deionized water until the pH level of CNTs attained to around 7. The soaked CNTs were then dried in vacuum oven (precision vacuum oven: Model 19) at 150 °C for 12 h. The average sizes of the CNT, AuNP and CuNP determined with transmission electron microscope (TEM) were 150–200 nm (length), 15 nm and 35 nm, respectively. CNTs in different volume fractions (0.2, 0.3, 0.5 and 0.8%) were added to water to produce CNT suspensions. The equivalent amount of CNTs by weight was

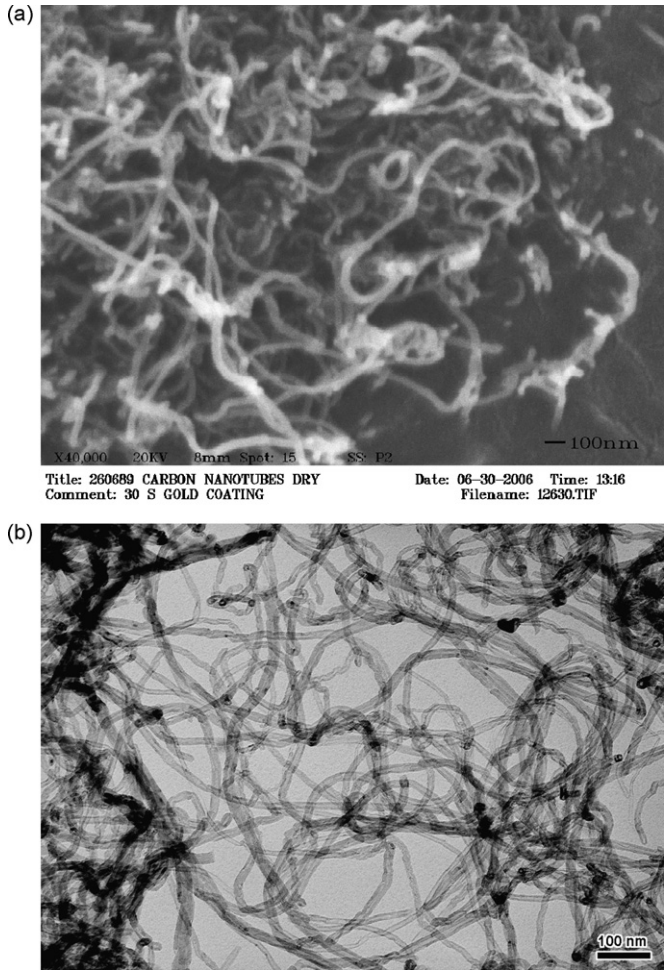

Fig. 1. (a) SEM image of the as-received CNTs and (b) TEM image of the as-received CNTs (in water).

measured in each case and was added to proportionate amount of water so that we could obtain the above CNT volume fraction in water. AuNP colloid was added to deionized water in the ratio of 1.4:1 by volume to produce AuNP suspension. AuNP suspension was added to different types of CNT suspensions having different volume fraction of CNTs, in 1.5–2.5 ratios to achieve CNT–AuNP suspensions.

In CuNP suspensions, the ingredients are CuNPs, laurate salt and deionized water. Laurate salt was added for stability of CuNPs in suspension. However, it was not as stable as was reported in Ref. [19]. Volume fractions of CuNPs were 0.05, 0.1, 0.2 and 0.3% with respect to water. The same procedure was used to achieve the proper volume fraction with respect to base fluid as it was done in CNT nanofluids. In each case, 9% of laurate salt by weight with respect to CuNP was added, to form the stabile CuNP suspensions. The reason is that repulsion forces between suspended CuNPs increase due to the increase of zeta potentials which denotes the surface charge of the CuNPs in fluid. Each type of CuNP suspension was added to a CNT suspension (0.5 vol.% CNT) in 1.5–2.5 ratios to produce CNT–CuNP suspension.

A Bransonic® Ultrasonic Cleaner 1510 (Branson Ultrasonics Corporation) was used as a low-power sonication to disperse the nanoparticles into water. Each type of suspension was sonicated for 1 h. Detailed information of the composition of suspensions with volumetric percentage and material properties is given in Table 1. Fig. 2 shows the TEM images of different suspensions. The thermal conductivity of suspensions was measured at room temperature (25 °C) using a TC-30 instrument from Mathis Co. This is a non-destructive thermal conductivity testing instrument which works on the modified hot wire technique. The instrument has an interfacial heat reflectance device and a constant heat source to the test materials comes from this device. The generated heat works in two ways. Part of it is absorbed by the materials and the rest takes part in raising the temperature at

Table 1
Samples of nanofluid suspensions for thermal conductivity tests

Single filler suspensions	Average size of particles (nm)	Density (g/cm^3)	Thermal conductivity at 300 K (W/(m K))	Descriptions	Volume fraction of nanoparticles (%)
CNTs	150–200	2.6	∼3000	CNTs + water	0.3 0.5 0.8
AuNPs	∼15	19.3	∼318	AuNP colloid + water	1.4
CuNPs	35–50	8.96	∼400	CuNPs + laurate salt + water	0.05 0.1 0.2 0.3

Hybrid fillers suspensions	Descriptions	Volume fraction of CNTs (%)	Volume fraction of other nanoparticles (%)
CNTs + AuNPs	CNTs + AuNP colloid + water	0.3 0.5	1.4 1.4
CNTs + CuNPs	CNTs + CuNPs + laurate salt + water	0.5 0.5 0.5 0.5	0.05 0.1 0.2 0.3

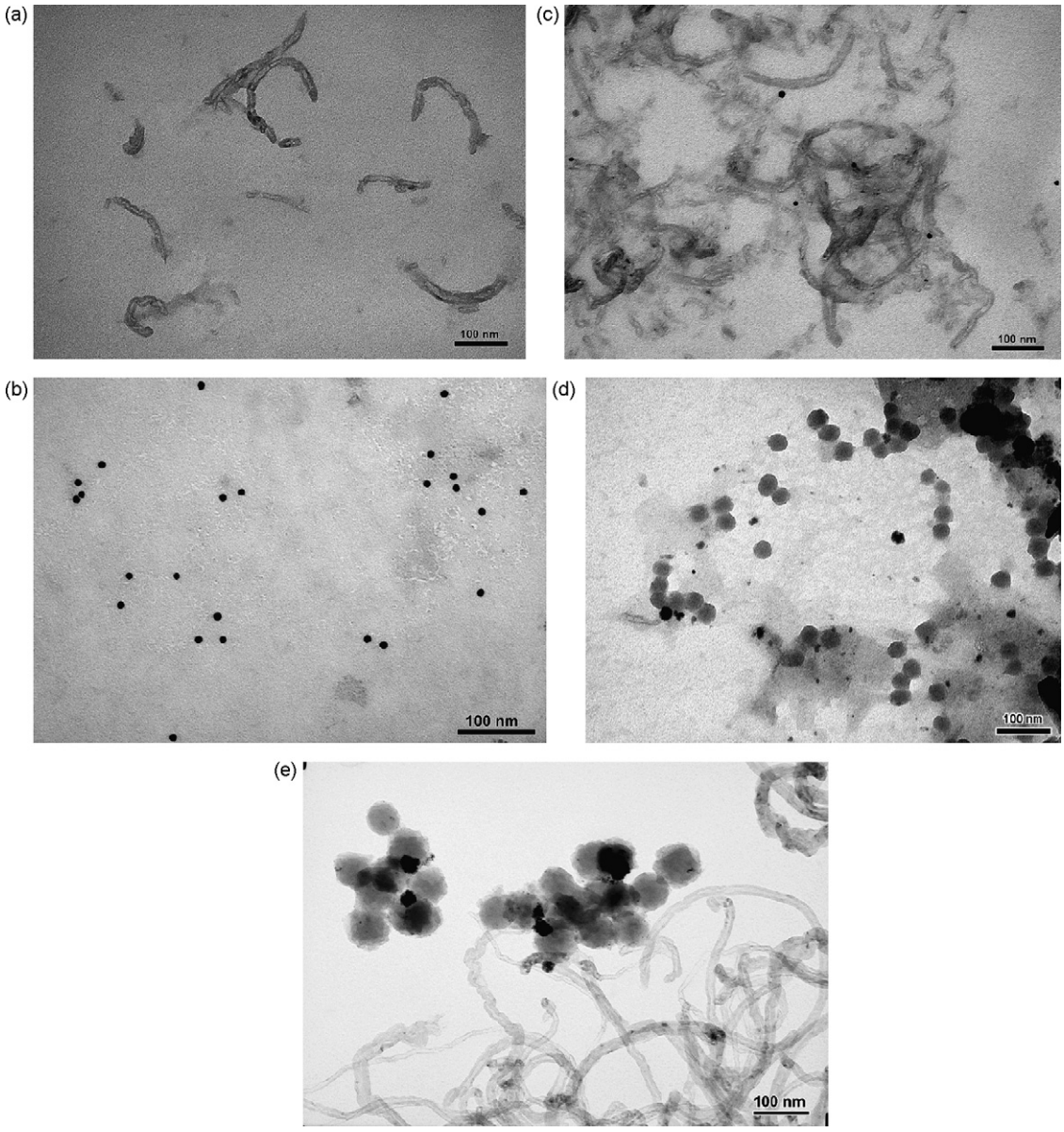

Fig. 2. (a) TEM image of CNTs (processed) in water suspension, (b) TEM image of AuNP suspension, (c) TEM image of AuNP–CNT suspension, (d) TEM images of CuNP suspension, and (e) TEM image of CuNP–CNT in water suspension.

the sensor interface. Heat transfer properties of the test sample are estimated from the rate of increase in temperature. Accuracy was more than 99%.

A glass plate was used for holding the suspensions. An area on the glass plate was chosen (as suggested by manufacturing company of the instrument) so that it can cover the sensor area fully and a barricade around the boundary of the area was made on the glass to hold the nanofluids. The silicon rubber paste was used to make the barricade and it took 24 h to be cured and solidified. The area was fixed and the amount of the fluid was also fixed such that it fully covered the sensor area and the height of nanofluid for each type of sample experiment was same. Before measuring the conductivity of nanofluids, the instrument was calibrated according to manufacturer instructions taking the glass plate fixture (with barricade) into account. Once a glass fixture had been used for measurement for one type of sample, it was cleaned completely with distilled water and then dried in the vacuum oven before proceeding to another kind of sample. To remove the influence of outer environment, the experiment setup was totally covered by a hard cover box. Test time for each sample was 2 s (as per manufacturer's guideline) which might be assumed as time of heat sourcing.

While measuring the thermal conductivity of different fluids especially CNT, CuNP suspensions, it was observed that poor dispersion and sedimentation of nanoparticles were prime obstacles in improvement of thermal conductivity of liquid. Therefore, we placed the sample of each kind in the experimental setup just after its bath sonication and analyses in this study have been made on the corresponding data obtained from the tests. To compare the effect of sedimentation/agglomeration on thermal conductivity, we also measured it in 5 min interval without any disturbance to specimens (this experiment were done with only

CuNP suspension of 0.3 vol.% CuNPs and CNT suspension of 0.8 vol.% CNTs).

The stability of the different nanofluids was measured with UV–vis–NIR spectrophotometer (Cary 5000, USA). Each type of nanofluid sample was scanned with scanning rate 600 nm/min in UV–vis–NIR spectrophotometer in each 5 min interval for half an hour to measure the suspension concentration with increasing sediment time. The wavelength range of light was 200–800 nm. To measure other parameters, in each case the absorbance at 252 was considered.

3. Results and discussion

3.1. Stability of nanofluid

Stability of a nanofluid used in practice is always extremely important. Therefore, stability of the prepared nanofluids was studied first. The experimental results from this thermal conductivity study of the nanofluids are expected to be a good reference for practical application if particle stability under sedimentation time shows a positive outcome. Stability of a nanofluid can be measured using UV–vis–NIR spectrophotometer, since at a particular wavelength; absorbance depends on the amount of nanoparticles in the nanofluid. The Beer–Lambert law expresses a linear relationship between an absorbance of light and the properties of a material through which light is passing. The law can be expressed in the following way:

$$A = \alpha l c \quad (1)$$

A is the absorbance, α the absorption coefficient (L in $\mathrm{mol}^{-1}\,\mathrm{cm}^{-1}$), l (cm) the distance that light travel through material and c is the concentration ($\mathrm{mol\,L}^{-1}$) of absorbing species in the material. This law is applicable to measure the absorbance of light in nanofluid [21–23]. Chemical and instrumental factors that limit the linearity of the Beer–Lambert law are generally very high concentrations and its electrostatic interaction at close proximity, shift in equilibrium as a function of concentration and fluorescence of the sample, etc. Due to polarity of the treated CNTs, electrostatic interactions between CNTs exist in their suspension; however, it does not work for other CuNP or AuNP suspensions. Other factors do not exist in any kind of suspensions.

Fig. 3 shows the absorbance of different nanofluids with variation of wavelength. The peak absorbance of CNT nanofluids appear at 252 and others at different wavelength. Fig. 4 shows the linear relationships between nanofiller concentrations and the absorbance of the suspended fillers of CNT (Fig. 4(a)), CuNP (Fig. 4(b)), CuNP–CNT (Fig. 4(c)) and AuNP–CNT (Fig. 4(d)). It can be seen that there was a slight deviation from linear behavior for CuNP nanofluid (Fig. 4(b)), while the other three showed clear linear relationships. However, reasons behind this phenomenon are unknown. It was also found that the absorbance is greater in CNT suspensions even with less concentration of CNTs compared to CuNP suspensions from the comparison of Fig. 4(a) and (b). Addition of CNTs into CuNP nanofluid improved the absorbance (Fig. 4(b) and (c)). It is possible that

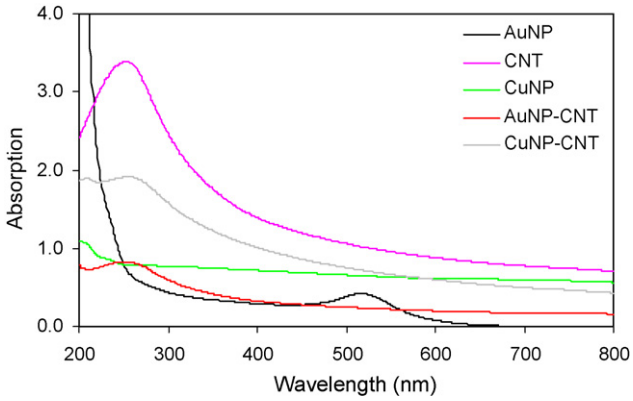

Fig. 3. UV–vis spectrum of different materials in water suspension.

the absorption coefficient of the material is mostly responsible for this behavior. In addition, other secondary parameters such as particle size, shape, dispersion, stability, etc. are also the keys in determining the absorption behavior. Higher exposed surface area of CNT compared to that of CuNP is another reason for higher absorbance in CNT suspension. Using this linear relationship, the relative stability of the nanofillers in the nanofluids with respect to sediment time was measured as shown in Fig. 5. Fig 5(a) compares the relative stability of all types of nanofluids with the same amount of nanofiller loading in each fluid. It is observed that the stability of CuNP nanofluid is poor, and within half an hour the concentration of the CuNPs in the fluid reduced to 85% compared to initial concentration level, whereas in the CNT nanofluid, the concentration decreased by 0.004% in same amount of time. Addition of CNTs into CuNP nanofluid reduced the sedimentation of CuNPs. Fig. 5(b) shows the relative stability of CNTs with time at different CNT loadings in the CNT nanofluid. It is observed that less CNT loading leads to more sedimentation. Various forces such as gravitational force on the particles, electrostatic force and van der Waals forces between particles are in effect in the nanofluid. It may be that due to fewer CNT nanoparticles, the distances between particles are much more than what is required to enable electrostatic and Van der Waals forces on them. Therefore, the effect of gravitational force, which favors sedimentation, is the dominant effect in the nanofluid with less CNT particles when compared to other forces. However, this characteristic was not found in CuNP nanofluids (Fig. 5(c)). In the CuNP nanofluid, gravitational force plays the major role in sedimentation, irrespective of the amount of CNT particles. In the AuNP–CNT nanofluid, the decrease of concentration is 0.008% (Fig. 5(e)); in the CuNP–CNT, the decrease is 0.016% (Fig. 5 (d)) within half an hour. The large specific area (surface area to volume) increases the stability of the suspension. In a nanofluid, gravity, Brownian forces and friction, forces may exist between nanoparticles and fluid. Since the CNTs we used in our experiment are polar nanofillers due to oxidation, they dispersed well in a polar media like the water we used for our study. Due to the polarization, CNTs have enhanced interactions with water molecules, and thus have better stability in the nanofluid. Since the density of CNTs is much smaller than that of CuNPs, the gravity effect on CNT sedimentation is less

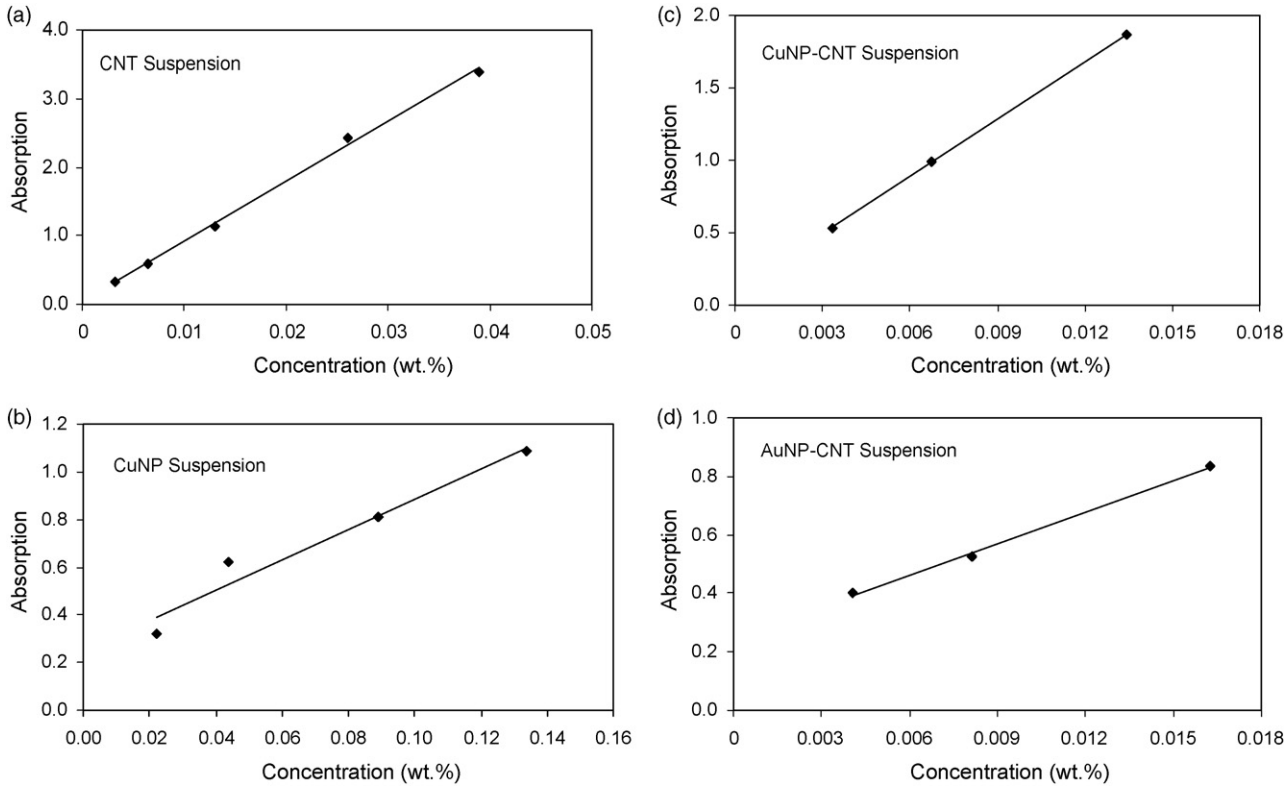

Fig. 4. (a) Linear relationship between light absorption and concentration of CNT suspension at wavelength of 252 nm. (b) Linear relationship between light absorption and concentration of CuNP suspension at wavelength of 252 nm. (c) Linear relationship between light absorption and concentration of CuNP in CuNP–CNT suspension at wavelength of 252 nm. (d) Linear relationship between light absorption and concentration of CNT in AuNP–CNT suspension at wavelength of 252 nm.

compared to that in CuNPs. We used AuNP colloid and therefore its sedimentation was expected to be much less.

3.2. Conductivity of nanofluids

The thermal conductivities of the nanofluids with single nanofillers, such as CNTs, CuNPs and AuNPs, were studied first.

The nanofluids with oxidized CNTs up to 0.8 vol.% with respect to water were prepared and tested to obtain the thermal conductivity. Fig. 6 shows the normalized thermal conductivity (ratio of thermal conductivity of CNT suspensions K_{eff} to thermal conductivity of the base fluid (water) K_w) as a function of volume fraction (%) of CNTs in water. The value of thermal conductivity of water was 0.613 W/(m K).

With the addition of CNTs, the thermal conductivity of the CNT suspensions increased notably with increase of the CNT volume fraction (%) in water. Thermal conductivity of the nanofluid with 0.8 vol.% CNTs showed 34% increase with respect to water. From the figure, it can be observed that the normalized thermal conductivity is non-linearly dependent on the volume fraction of CNTs.

Assael et al. [11] reported the similar results to that found in our experiment with CNT suspension. Choi et al. [4] worked on CNTs/oil nanofluid as well as water and observed better results with a 110% increase of nanofluid thermal conductivity over water with the addition of 0.8% CNTs by volume. Oil is more viscous compared to water and therefore with good dispersion of CNT in CNT–oil nanofluid, greater stability of CNT is achieved in oil compared to that in water. Size and shape of CNTs may be the main factors for the non-linear relationship of thermal conductivity and CNT loadings. The results imply that CNTs interact with each other due to their high aspect ratio, even with low CNT loading.

The change of thermal conductivity of nanofluid with CuNPs compared to water was tested (Fig. 7) and as expected, the addition of CuNPs showed an increase of the thermal conductivity. From Fig. 7, it can be observed that normalized thermal conductivity of the CuNP suspension increases with increase of CuNP volume fraction (%). With CuNP concentration of 0.3% by volume, an increment was around 74% at room temperature over water. Unlike CNT nanofluid, normalized thermal conductivity of the CuNP nanofluid shows linear dependency on CuNP volume fraction (%). This result obtained in our experiment presents better enhancement compared to 40% increment for the nanofluid consisting of ethylene glycol containing 0.3% CuNP by volume [14]. Comparing other's research work regarding thermal conductivity of nanofluids, it can be said that the size of Cu nanoparticles (~35–50 nm) and especially better dispersion (due to instant bath sonication) were the reasons behind this vast improvement.

For the nanofluid with AuNPs, only a fixed volume fraction of AuNP was added to water to measure changes of the thermal conductivity. Based on this, nanofluids with hybrid nanoparticles were then studied. To observe the effect of CNTs on thermal conductivity of AuNP suspensions, CNTs in different concentration

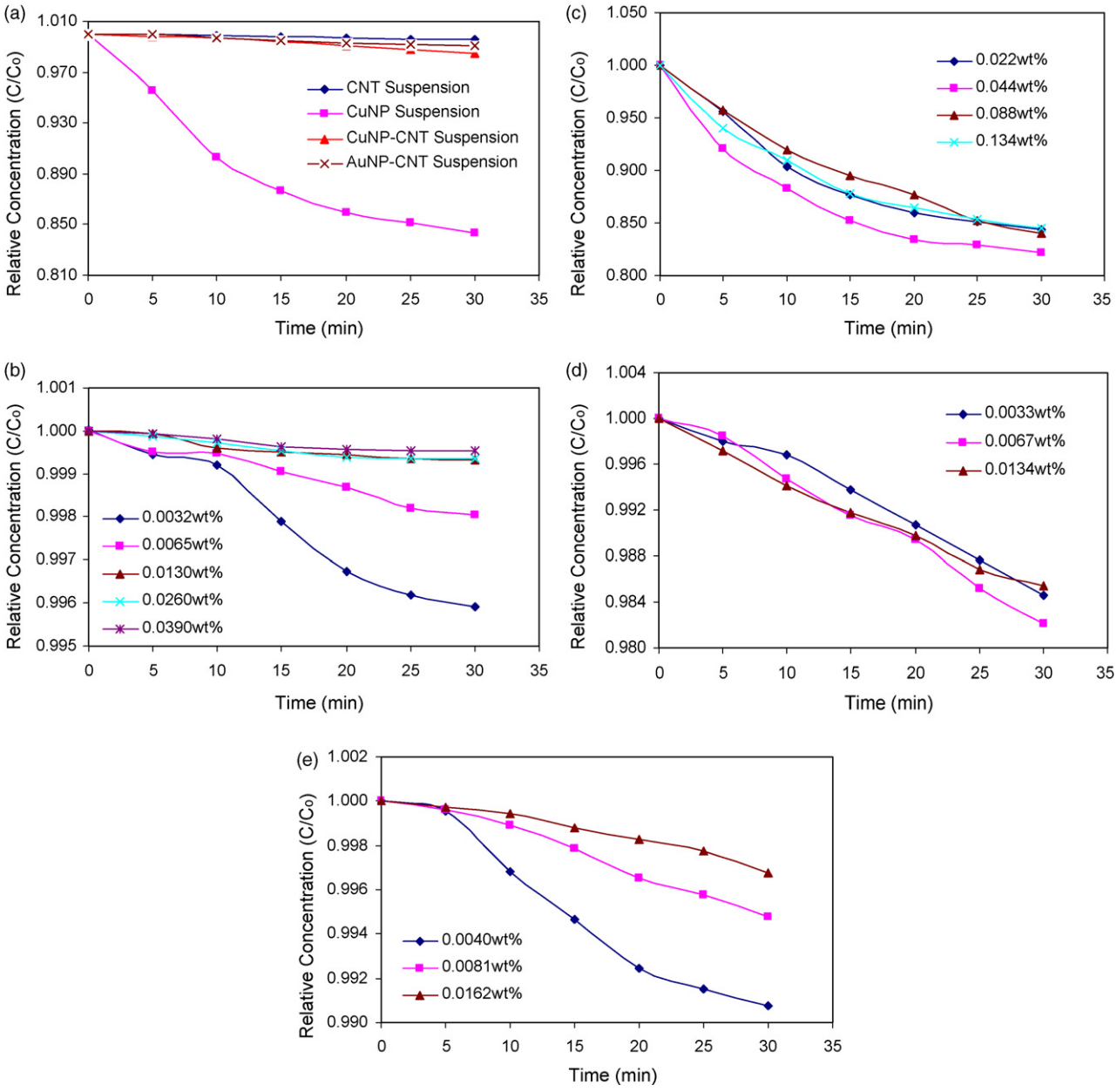

Fig. 5. (a) Relative supernatant particle concentration of nanofluids with sediment time. (b) Relative supernatant CNT concentration of CNT nanofluids with sediment time. (c) Relative supernatant CuNP concentration of CuNP nanofluids with sediment time. (d) Relative supernatant CuNP concentration of CuNP–CNT nanofluids with sediment time. (e) Relative supernatant CNT concentration of AuNP–CNT nanofluids with sediment time.

were added to AuNP suspensions. Fig. 8 shows the normalized thermal conductivity values of AuNPr and CNT–AuNP nanofluids as a function of volume fraction (%) of CNTs and AuNPs in water. It can be found that the nanofluid with 1.4 vol.% AuNP colloid showed 37% increment in thermal conductivity over water. The addition of CNTs to AuNP nanofluid with 1.4 vol.% AuNP colloid does not show obvious improvement of thermal conductivity. Since the particle size of AuNPs was smaller than the size of CuNPs, the AuNP nanofluid should have higher conductivity compared to CuNP nanofluid due to surface to volume ratio, however the experimental results did not show that. For higher thermal conductivity of nanofluid, higher exposed surface area of nanoparticles, good network between them and stability of network are required. In the AuNP suspension, the first and third criteria were fulfilled but due to fewer nanoparticles per unit volume compared to that in CuNP suspension (as found in TEM images), there was a lack of good network and resulted in lower thermal conductivity.

Beside the AuNP–CNT hybrid nanofluid (fixed AuNP concentration, varied CNT concentration), CuNP–CNT hybrid nanofluid was prepared with fixed amount of CNTs and varied CuNP concentrations to measure the effect on thermal conductivity of the suspensions. All the concentrations were in volume fraction. Fig. 9 shows the effect of CNTs added to CuNP nanofluids at room temperature. CNTs did not increase the thermal conductivity of the CuNP–CNT nanofluid but rather lowered the

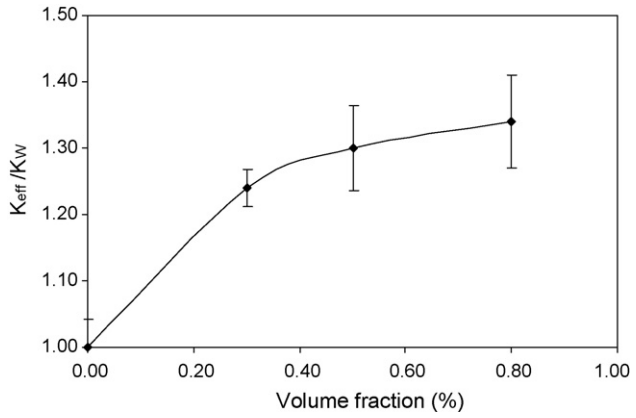

Fig. 6. Normalized thermal conductivity of CNT suspensions as a function of CNT concentration.

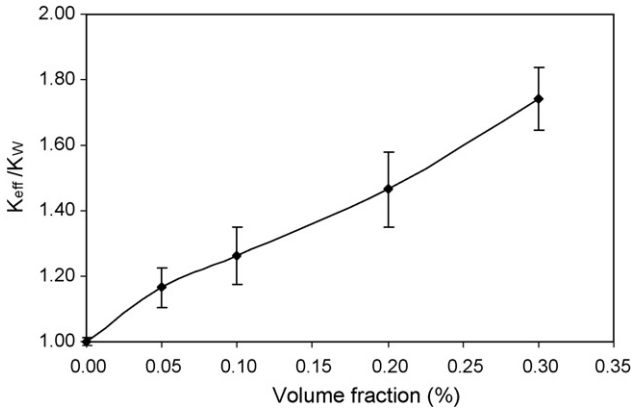

Fig. 7. Normalized thermal conductivity of CuNP nanofluids as a function of CuNP concentration.

values if compared to thermal conductivity of respective single CuNP nanofluids. Even with increased amounts of the CuNPs in CuNP–CNT suspension, thermal conductivity decreases, and standard deviation increases. The same phenomena were also found in AuNP–CNT suspensions. The standard deviation was very high due to the addition of CNTs in these hybrid nanofluids. However, nanofluid with only CNTs did not show high standard deviation. Therefore, the synergistic effect of hybrid nanofluid

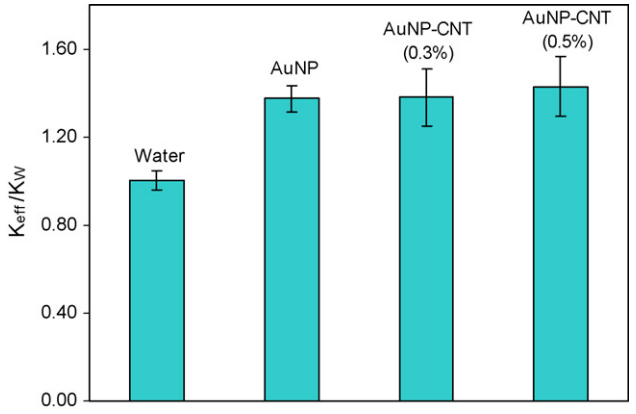

Fig. 8. Normalized thermal conductivity of nanofluids as a function of AuNP and CNT concentrations.

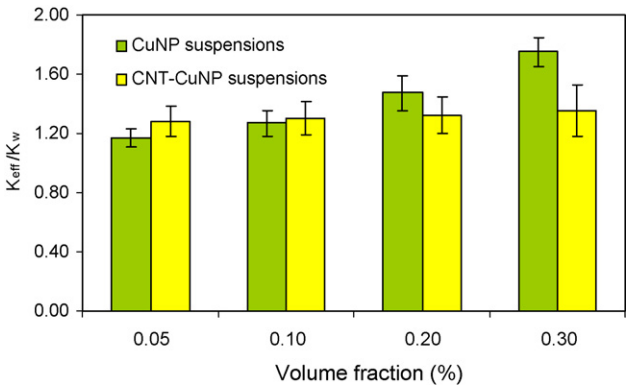

Fig. 9. Comparison of normalized thermal conductivity between CuNP suspensions and CNT–CuNP suspensions as a function of CuNP concentration.

that was expected to produce higher thermal conductivity did not occur.

To compare the effect of sedimentation on thermal conductivity, its measurements in 5-min interval were conducted without any disturbance to specimens (only 0.3 vol.% CuNP suspension and 0.8 vol.% CNT suspension). Fig. 10 shows the vast decrease of their thermal conductivity with respect to sedimentation time. It can be observed that in 5-min interval, thermal conductivity improvement was reduced from 74% to 30%, 16% and 10% for CuNP and from 30% to 5%, 2% and 1% for CNT. Therefore, solving this sedimentation problem is an important factor to achieve high thermal conductivity of liquid and in reality this job is a difficult one to perform as observed by other researchers too. Comparing Fig. 5 (b), (c) and 10, it can be said that agglomeration rather than sedimentation might be the possible reason for the decrease in thermal conductivity of CNT suspension. In case of CuNP, both sedimentation and agglomeration might be responsible for reduction of thermal conductivity with respect to time.

3.3. Verification of measured data with existing macroscopic models

Several macroscopic models which were developed about a century ago were considered for comparison of the experimen-

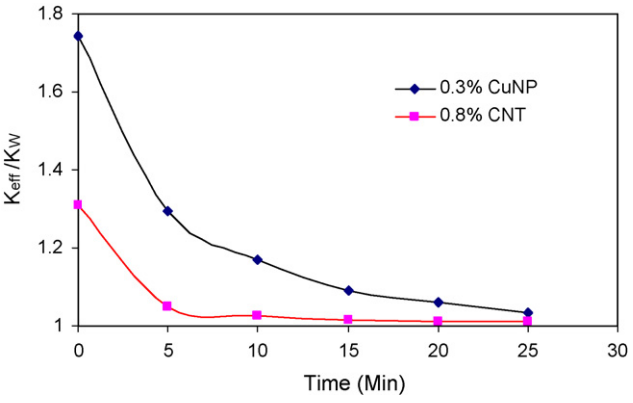

Fig. 10. Normalized thermal conductivity of CuNP and CNT nanofluids as a function of sedimentation time.

tal results with theoretical predictions for thermal conductivities of the nanofluids containing CNTs or CuNPs in water. All such models are founded in Fourier's law of heat conduction applied to both media. We calculated the thermal conductivity of nanofluids containing CuNPs in water suspensions using Maxwell [24], Hamilton–Crosser [25], Jeffery [26], Davis [27] and Lu–Lin [28] models. Those models are given below:

$$\frac{k_{\text{eff}}}{k_{\text{w}}} = 1 + \frac{3(\alpha-1)\phi}{(\alpha+2)-(\alpha-1)\phi} \quad \text{(Maxwell)} \tag{2}$$

spherical particle are considered. Accurate to order ϕ^1, applicable to $\phi \ll 1$ for $|\alpha - 1| \ll 1$.

$$\frac{k_{\text{eff}}}{k_{\text{w}}} = \frac{\alpha + (n-1) - (n-1)(1-\alpha)\phi}{\alpha + (n-1) + (1-\alpha)\phi} \quad \text{(Hamilton–Crosser)} \tag{3}$$

spherical and non-spherical particles are considered: $n = 3$ for spheres and $n = 6$ for cylinders. Accurate to order ϕ^1, applicable to $\phi \ll 1$ for $|\alpha - 1| \ll 1$.

$$\frac{k_{\text{eff}}}{k_{\text{w}}} = 1 + 3\beta\phi + \left(3\beta^2 + \frac{3\beta^3}{4} + \frac{9\beta^3}{16}\frac{\alpha+2}{2\alpha+3} + \frac{3\beta^4}{2^6} + \cdots\right)\phi^2 \quad \text{(Jeffrey)} \tag{4}$$

accurate to order ϕ^2, high-order terms represent pair interactions of randomly dispersed spheres.

$$\frac{k_{\text{eff}}}{k_{\text{w}}} = 1 + \frac{3(\alpha-1)}{(\alpha+2)-(\alpha-1)\phi}[\phi + f(\alpha)\phi^2 + 0(\phi^3)] \quad \text{(Davis)} \tag{5}$$

accurate to order ϕ^2, high-order terms represent pair interactions of randomly dispersed spheres. $f(\alpha) = 2.5$ for $\alpha = 10$; $f(\alpha) = 0.5$ for $\alpha = \infty$.

$$\frac{k_{\text{eff}}}{k_{\text{w}}} = 1 + a\phi + b\phi^2 \quad \text{(Lu–Lin)} \tag{6}$$

spherical and non-spherical particles are considered. For spherical particles, $a = 2.25$, $b = 2.27$ for $\alpha = 10$; $a = 3.00$, $b = 4.51$ for $\alpha = \infty$. Near- and far-field pair interactions are considered.

The above models are suitable for nanofluid having spherical or rotational elliptical particles with small axial ratio M ($M = a/b$). The a, b and c ($c = b$) are the semi-radii along x, y and z axes, respectively. CuNPs can be considered as spherical and all the existing models might work for CuNP suspensions. Fig. 11 shows that the theoretical results from the existing models which are much lower than the experimental data shown in Fig. 9 (if both experimental and theoretical results are shown in the same figure, the behavior of theoretical results could not be conveyed) Thermal conductivity of CuNPs (k_{p}) has been considered as 385 W/mK [8]. For water (k_{w}), it is 0.613 W/(m K). Hamilton–Crosser [25] and Lu–Lin [28] models also consider the cylindrical shape of the nanoparticle and can be used for CNT suspensions. The results from this model (Fig. 12) for CNT ($k = 3000$ W/(m K)) suspension also present the same behavior compared to their experimental data (Fig. 6) as CuNP provides. The fact that experimental data are much higher than the theoretical result in each case indicated that the conventional models

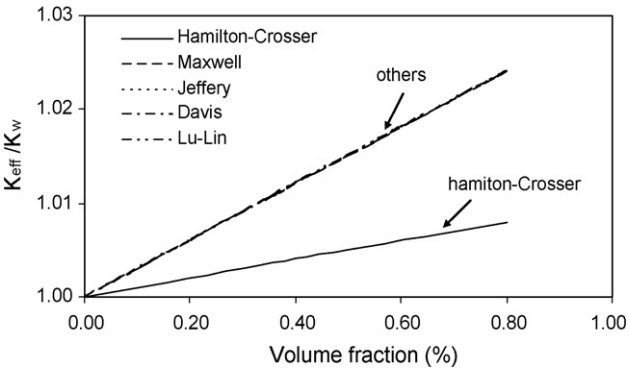

Fig. 11. Calculated thermal conductivity of CuNP suspensions by the conventional models.

cannot predict thermal conductivity of the nanofluids, i.e. effective macro-scale medium theory is not applicable in explaining the thermal transport in the nanofluids.

However, CNTs can be considered as rotational elliptical nanoparticles having a very large axial ratio $M \gg 1$. Therefore, existing models cannot represent CNT-based nanofluids. Additionally, the space distribution of CNTs has some effect on conductivity and this issue has not been considered in these models. Xue [29] has a new model considering very large axial ratio and space distribution of CNTs. Generally CNTs are randomly distributed in the fluid unless special arrangements such as the use of magnetic fields, etc. are applied. The expression of the effective thermal conductivity of CNTs-based nanofluid considering effect of distribution state of CNT is

$$\frac{k_{\text{eff}}}{k_{\text{w}}} = \frac{1-\phi+(4\phi/\pi)\sqrt{k_{\text{p}}/k_{\text{w}}}\arctan(\pi/4\sqrt{k_{\text{p}}/k_{\text{w}}})}{1-\phi+(4\phi/\pi)\sqrt{k_{\text{w}}/k_{\text{p}}}\arctan(\pi/4\sqrt{k_{\text{w}}/k_{\text{p}}})} \quad \text{(Xue)} \tag{7}$$

Xue [29] modified the Maxwell model [24] by adding the effect of space distribution of CNTs in the fluid and it is found that the distribution state of CNTs in water suspension has a big effect on thermal conductivity of CNT nanofluid. Considering the values of thermal conductivity of CNTs (k_{p}) as 900–3000 W/(m K) [28], it is found that the experimental data are not in good agreement with these newer theoretical approaches (Fig. 13). Therefore, a new model needs to be developed. However, it is

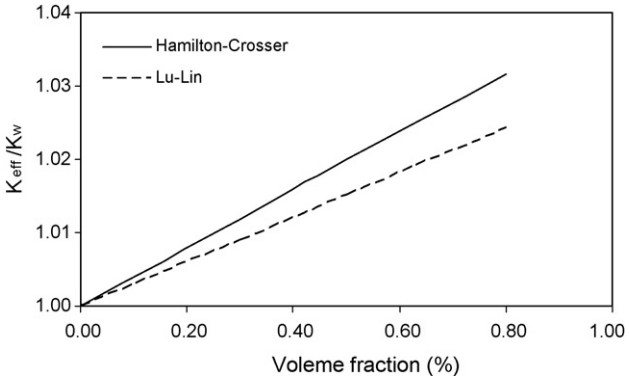

Fig. 12. Calculated thermal conductivity of CNT suspensions by the conventional models.

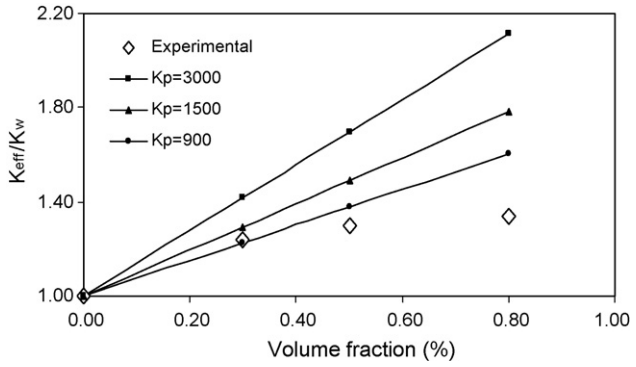

Fig. 13. Comparison between the calculated thermal conductivity of CNT suspensions and experimental data.

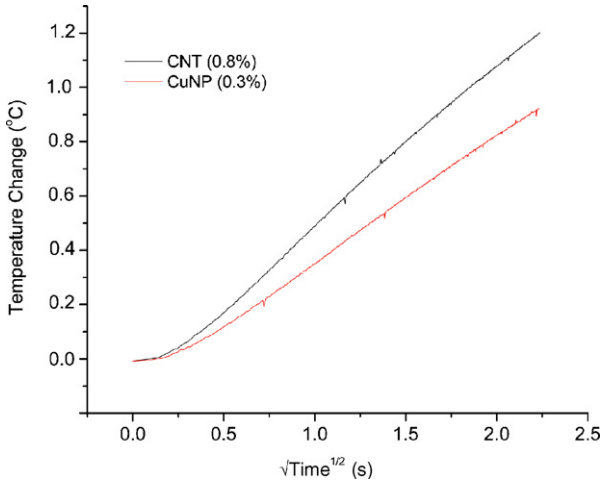

Fig. 14. Temperature change (°C) vs. square root of time plot.

difficult to consider how to implement the factors discussed in next section, in such new models, which influence the thermal conductivity.

3.4. Correlation of test results and heat transfer mechanism

Fig. 6 shows that the normalized thermal conductivity of CNT nanofluid is non-linear with respect to volume fraction of nanotubes. Geometric anisotropy caused by large aspect ratios of nanotubes, and physical anisotropy originating from interfacial thermal resistance, are the reasons for the non-linear behavior [30]. The shape of particles in a nanofluid is also a major factor in thermal conductivity determination. Even though from the TEM images, it is observed that the particles are of particular shape and size, due to their agglomeration, which increases with the increase of loading, the final shape and size are unpredictable. The effect on shape and size due to agglomeration might be a cause of non-linearity of conductivity with loading.

Enhancement of thermal conductivity of CNTs suspension might come from improved dispersion of CNTs (due to oxidization/polarization of CNTs) and good contact among them (Fig. 1(b)). Other factors e.g. phase system in nanofluid might play a role. Surfactants present in nanofluids can alter their viscosity which can cause the reduction of temperature gradient or timescale for the onset of natural convection currents in nanofluids. In addition, due to the existence of more than one phase in nanofluid, settling of the particles may induce natural convection currents earlier as compared to the prediction by single-phase theory, thus unstable nanofluids can easily induce premature convective currents. Similar to CNTs, AuNP and CuNP suspensions showed higher thermal conductivity values, possibly also due to the good dispersion of nanoparticles and phase system in the nanofluids.

To find out the way of heat transfer, temperature change (°C) versus square root of time plot were analyzed. Fig. 14 shows the temperature change versus square root of time plot for 0.8 vol.% CNT and 0.3 vol.% CuNP suspensions (as obtained in the test). This indicates the temperature rise occurring at the contact surface of specimen and sensor during the test. From the figure it can be observed that at the beginning the curve is non-linear and the rests are linear. It means that at the very beginning of test, natural convection and other natural settling-induced convection might play a role in thermal conduction and rest were performed by the conduction. Therefore, it can be said that the thermal conductivity values measured in this experiment were mostly conductive values. In addition, it can be said that instant bath sonication did not influence the thermal convection in the system.

However, thermal conductivity of the AuNP suspension was not improved with addition of CNTs possibly due to a lack of collaboration between AuNPs and CNTs. Thermal conductivity in the CuNP–CNT suspension also decreased compared to that in CuNP suspension. The possible reason is again surmised as poor collaboration between CuNPs and CNTs (Fig. 1(g)) and hence more thermal interfacial resistance evolved. And possibly the addition of CNTs into the CuNP suspension degraded the dispersion of both types of nanomaterials resulting in increased agglomeration. This observation can be made by comparing Fig. 1(c), (f) and (g). This agglomeration might be the root cause of the decrease in thermal conductivity of CuNP–CNTs nanofluids. Another possible reason is that CNTs are less prone to convection due to their stability and addition of them to CuNP suspension inhibits the natural convection currents causing the lowering of conductivity of CuNP suspension.

More experiments should be conducted to elucidate the mechanisms behind these enhancements of thermal conductivity and new theories are clearly in need to interpret the mechanisms for the thermal conductivity enhancement of the nanofluids which include considerations of several factors, including viscosity of the base fluid, stability of the nanoparticles in the suspension fluids and characteristics of the nanofillers (size, aspect ratio, specific area, etc.) which are not included in the existing models.

4. Conclusions

Nanofluids containing single CNTs, CuNPs and AuNPs separately and hybrids of them were prepared in water and their thermal conductivities were measured. Enhancement in thermal conductivity of CNT, AuNP and CuNP suspensions was observed, whereas the hybrid nanofluids with CNT–AuNP and CNT–CuNP did not improve the thermal conductivity, which

indicated that there was no positive synergistic effects found in these tests. Among all types of nanofluids, nanofluid with CuNPs showed the best result (about 74% increment over the base fluid), and the increase of CuNP concentration in CuNP suspension showed a linear relationship with thermal conductivity enhancement. In the CNT suspension, enhancement was non-linearly dependent on amount of CNT. CNT-based nanofluids showed higher stability compared to CuNP nanofluid. However, both CuNP and CNT suspensions showed the drastic decrease of their thermal conductivity with time variation due to sedimentation and agglomeration. Existing theoretical models did not match well with the experimental data in this study. Further studies and analyses need to be performed to achieve an understanding of the mechanisms and effective models for prediction of enhancement in thermal conductivity need to be developed. Successful application of high thermal conductive nanofluid could bring advantages to industry by decreasing the scale and energy consumption of cooling systems.

Acknowledgements

The authors are very grateful to Mr. Russell G. Maguire of the Boeing Company for fruitful discussions on this work. The authors gratefully acknowledge the support from NSF through NIRT grant 0506531. This work is also partially supported by NASA through grant NNM04AA62G. We are grateful to Dr. Wayne Reitz for providing us with the copper nanoparticles. Mr. Gerry L. Scherbenske was also involved in the test work of this study.

References

[1] S.U.S. Choi, Proceedings of the American Society of Mechanical Engineers (ASME), vol. 66, ASME, New York, NY, 1995, p. 99.
[2] S. Lee, S.U.S. Choi, S. Li, J.A. Eastman, Measuring thermal conductivity of fluids containing oxide nanoparticles, ASME J. Heat Transfer 121 (1999) 280.
[3] X. Wang, X. Xu, S.U.S. Choi, J. Thermophys. Heat Transfer 13 (1999) 474–480.
[4] S.U.S. Choi, Z.G. Zhang, W. Yu, F.E. Lockwood, E.A. Grulke, Appl. Phys. Lett. 79 (2001) 2252–2254.
[5] Y. Xuan, Q. Li, Int. Heat Fluid Flow 21 (2000) 58–64.
[6] P. Keblinski, S.R. Phillpot, S.U.S. Choi, J.A. Eastman, Int. J. Heat Mass Transfer 45 (2002) 855–863.
[7] S. Iijima, Nature 354 (1991) 56–58.
[8] P. Kim, L. Shi, A. Majumdar, P.L. McEuen, Phys. Rev. Lett. 87 (2001), 215502/1-15502/4.
[9] S. Berber, Y.K. Kwon, D. Tomanek, Phys. Rev. Lett. 84 (2000) 4613–4616.
[10] H. Xie, H. Lee, W. You, M. Choi, J. Appl. Phys. 94 (2003) 4967–4971.
[11] M.J. Assael, C.F. Chen, I. Metaxa, W.A. Wakeham, Int. J. Thermophys. 25 (2004) 971–985.
[12] H. Masuda, A. Ebata, K. Teramae, N. Hishinuma, Netsu Bussei 4 (1993) 227–233.
[13] L.P. Zhou, B.X. Wang, Annu. Proc. Chin. Eng. Thermophys. (2002) 889–892.
[14] J.A. Eastman, S.U.S. Choi, S. Li, W. Yu, L.J. Thompson, Appl. Phys. Lett. 78 (2001) 718–720.
[15] R.L. Hamilton, O.K. Crosser, Ind. Eng. Chem. Fundam. 1 (1962) 187–191.
[16] H.E. Patel, S.K. Das, T. Sundararajan, A.S. Nair, B. George, T. Pradeep, Appl. Phys. Lett. 83 (2003) 2931–2933.
[17] S.K. Das, N. Putra, P. Theisen, W. Roetzel, ASME J. Heat Transfer 125 (2003) 567–574.
[18] K. Esumi, M. Ishigami, A. Nakajima, K. Sawda, H. Honda, Carbon 34 (1996) 279–281.
[19] Y. Xuan, Q. Li, Int. J. Heat Fluid Flow 21 (2000) 58–64.
[20] M.S. Liu, M.C. Lin, C.Y. Tsai, C.C. Wang, Int. J. Heat Mass Transfer 49 (2006) 3028–3033.
[21] J.G. Smith, J.W. Connell, K.A. Watson, P.M. Danehy, Polymer 46 (2005) 2276–2284.
[22] V. Golob, L. Tusek, Dyes Pigments 40 (1999) 211–217.
[23] R. Peixoto et al., Light transmission through porcelain, Dent. Mater., 2007, doi:10.1016/j.dental.2006.11.025.
[24] J.C. Maxwell, A Treaties on Electricity and Magnetism, 2nd ed., Oxford University Press, Cambridge, UK, 1904, 435.
[25] R.L. Hamilton, O.K. Crosser, Thermal conductivity of heterogeneous two-component systems, industrial and engineering chemistry, Fundamentals 1 (1962) 187–191.
[26] D.J. Jeffery, Proc. Roy. Soc. London A 335 (1973) 355–367.
[27] R.H. Davis, Int. J. Thermophys. 7 (1986) 609–620.
[28] S. Lu, H. Lin, J. Appl. Phys. 79 (1996) 6761.
[29] Q.Z. Xue, Physica B 368 (2005) 302–307.
[30] L. Gao, X.F. Zhou, Phys. Lett. A 348 (2006) 355–360.